Before the second glance: neural correlates of refixation planning in precursor fixations

Andrey R. Nikolaev[1,2]*, Benedikt V. Ehinger[3], Radha Nila Meghanathan[4], Cees van Leeuwen[2,5]

[1] Department of Psychology, Lund University, Lund, Sweden
[2] Brain & Cognition Research Unit, KU Leuven - University of Leuven, Leuven, Belgium
[3] Stuttgart Center for Simulation Science, University of Stuttgart, Germany
[4] Department of Experimental Psychology, Otto-von-Guericke University Magdeburg, Germany
[5] Center for Cognitive Science, Technical University, Kaiserslautern, Germany

* Corresponding author
Department of Psychology,
Lund University,
Box 213
22100 Lund
Sweden
andrey.nikolaev@psy.lu.se

Abstract

Eye tracking studies of refixation behavior have suggested that refixations serve to recover information lost or missed during continued exploration of a visual scene. These studies have largely ignored precursor fixations, the first fixations on locations that later refixations return to. To examine the neural mechanisms of precursor fixations, we analyzed simultaneously recorded EEG and eye movement in a free-viewing contour search task. We compared fixation-related EEG activity in three categories of fixations: ordinary fixations on locations that were visited only once, refixations, and precursor fixations. We developed a methodological pipeline involving regression-based deconvolution modeling to account for overlapping EEG responses due to the saccade sequence and other oculomotor covariates. We found that precursor fixations were preceded by the largest saccades among the fixation categories. Independently of the effect of saccade length, EEG amplitude was enhanced in precursor fixations, compared to the other fixation categories 200-400 ms after fixation onsets, most noticeably over the occipital areas. Our findings reflect the neural mechanisms underlying the most basic categories of fixation behavior, highlighting the strategic role of precursor fixations in visual exploration. The methodological pipeline presented here offers a broadly applicable tool for investigating perceptual and cognitive processes in naturalistic viewing.

Keywords: naturalistic viewing behavior, gaze revisits, electroencephalography, visual search, healthy adults

Introduction

In natural viewing, the eyes often return to locations that were visited several seconds before (Yarbus, 1967). Such returns, or refixations, constitute up to 35% of eye movements (Beck, Peterson, & Vomela, 2006; Mannan, Ruddock, & Wooding, 1997; Zelinsky, Loschky, & Dickinson, 2011). Their prevalence raises the question of what their role might be. This question has made them a subject of intensive eye-tracking research (Gilchrist & Harvey, 2000; Körner & Gilchrist, 2008; Shen, McIntosh, & Ryan, 2014; Tatler, Gilchrist, & Land, 2005; Zelinsky et al., 2011).

Research so far has predominantly concentrated on refixations and ignored the potentially equally important fixation category of first fixations on locations to which the gaze later returns. Let us call these *precursor* fixations (Fixation 1 in Fig. 1). We know of only one study in which this category of fixations has been addressed (Wilming, Harst, Schmidt, & König, 2013). The authors found that, compared to fixation locations the eyes do not return to, precursor fixation locations were more visually salient and fixated longer. Wilming and colleagues suggest that these locations carry information that warrants additional scrutiny but nonetheless, priority is given to further exploration. This prompts the eyes to move on, making a later revisit inevitable. However, revisits may be needed for different reasons as well. Perhaps, these locations remain salient during exploration and hence likely to continue attracting fixations. Or perhaps the eyes return because salient information was forgotten. Although little is known about the selection and acquisition of visual information at precursor fixation locations, it is likely to differ from ordinary fixations in ways yet to be explored.

Our current investigation is focused on the neural signals that are associated with precursor fixations. We study precursor fixations using simultaneously recorded eye movement and EEG. Doing so enables unrestricted viewing tasks, which have greater ecological validity than more traditional tasks in which the eyes are fixed during stimulus presentation. Consequently, experimental paradigms with unrestricted eye movement behavior have been used, among others, to study reading (Dimigen, Sommer, Hohlfeld, Jacobs, & Kliegl, 2011), memory encoding (Nikolaev, Nakatani, Plomp, Jurica, & van Leeuwen, 2011), visual search (Kamienkowski, Varatharajah, Sigman, & Ison, 2018; Körner et al., 2014), perception of natural scenes (Coco, Nuthmann, & Dimigen, 2020; Devillez, Guyader, & Guerin-Dugue, 2015), aesthetic evaluation of art (Fudali-Czyz, Francuz, & Augustynowicz, 2018), and decision making in product valuation (Tyson-Carr et al., 2020). However, none of these studies considered refixations or precursor fixations.

By focusing on precursor fixations, the current investigation complements two of our previous studies. Both studies were focused on refixations rather than on precursor fixations. Like the current one, they used EEG-eye movement co-registration in visual search tasks. In the first (Nikolaev, Meghanathan, & van Leeuwen, 2018), of which the data are also used in the current analysis, participants searched for a collinear contour among a field of randomly oriented Gabor elements. Nikolaev et al. (2018) focused on presaccadic potentials time-locked to the saccade onset (saccade-related potentials, SRPs). Presaccadic potentials indicate saccade planning and preparation, including the shift of attention to the next saccade target (Kovalenko & Busch, 2016; Nikolaev, Jurica, Nakatani, Plomp, & van Leeuwen, 2013; Wauschkuhn et al., 1998). The presaccadic potential was found to be reduced in amplitude for refixations compared to ordinary fixations over the parieto-occipital regions. The difference may indicate a refixation mechanism operating at the saccade planning stage. The same study also examined postsaccadic potentials. These, time-locked to fixation onset (fixation-related potentials, FRPs), reflect initial encoding of visual information at

fixation (Kamienkowski et al., 2018; Kazai & Yagi, 2003; Ries, Touryan, Ahrens, & Connolly, 2016). We found a difference in FRP amplitude over the occipital regions about 270 ms after fixation onset between ordinary fixations and refixations. However, this difference was also observed between control fixation pairs (fixations 2 and 4 in Fig. 1), which preserve only the fixation rank (the order of fixations within a trial), but not the actual relationship in the pairs. We interpreted this result as evidence that apart from the effect of fixation order on FRP amplitude, information acquisition at refixations proceeded indistinguishably from ordinary fixations.

In a second study (Meghanathan, van Leeuwen, Giannini, & Nikolaev, 2020), participants searched for multiple target Ts among a field of distractor Ls, all in different orientations. There were 3, 4 or 5 targets and their orientations were to be remembered for subsequent change detection. We compared presaccadic potentials between first fixations and refixations on targets and distractors. For targets only, presaccadic potential amplitude over the occipital regions was higher for first fixations than for refixations. Saccade planning of refixations, therefore, is modulated by top-down factors such as task-relevance.

While both studies identify distinct factors affecting the saccade planning processes immediately prior to a refixation, neither of them provides us with any information regarding precursor fixations. The ordinary fixations in Nikolaev et al. (2018) and first fixations in Meghanathan et al. (2020) are pooled categories, encompassing both precursor fixations and fixations not followed by any refixation (fixations 1, 2, 4 in Fig. 1). The same pooling leaves inconclusive Nikolaev's et al. (2018) observation that, once the eyes have landed on the revisited location, information acquisition proceeded indistinguishably from ordinary fixations. Thus, an analysis of precursor fixations is crucial in order to understand what happens, not only at the time of the precursor fixation, but also at the time of the refixation.

To examine the neural mechanisms of visual information processing at precursor fixation locations, we compare the amplitude of postsaccadic FRP between three fixation categories: ordinary fixations, refixations, and precursor fixations (Fig. 1). We focus on two time windows: the first one captures the lambda wave about 100 ms after fixation onset, which is seen as an early perceptual response of the visual cortex (Dimigen, Valsecchi, Sommer, & Kliegl, 2009; Kazai & Yagi, 1999; Ossandón, Helo, Montefusco-Siegmund, & Maldonado, 2010; Thickbroom, Knezevic, Carroll, & Mastaglia, 1991); the second window captures the late FRP wave after 200 ms, where we observed the FRP effect indicating differences in information uptake over the time course of visual exploration (Nikolaev et al., 2018). In line with the late FRP effects found over the occipital region (Fischer, Graupner, Velichkovsky, & Pannasch, 2013; Nikolaev et al., 2018), we expect to observe fixation category differences in FRP over the occipital areas.

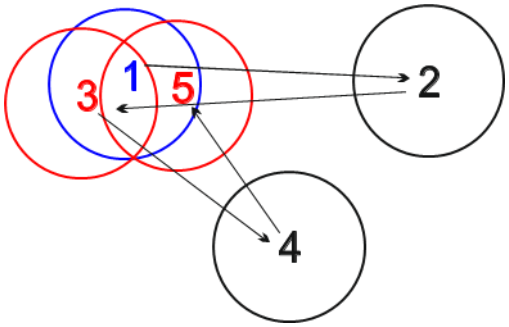

Fig. 1. Fixation categories. Numbers indicate fixation rank, i.e., the position in the order of fixations within a trial. Circles represent areas within a radius of 2° of visual angle around the fixation point. We consider fixation 1 as a precursor fixation; fixations 2 and 4 as ordinary fixations; fixations 3 and 5 as refixations. In our previous studies, we did not distinguish between precursor fixations and ordinary fixations. In (Nikolaev et al., 2018), we considered fixations 1, 2 and 4 as ordinary fixations and fixations 3 and 5 as refixations. Similarly, in another previous study (Meghanathan et al. 2020), we considered fixations 1, 2 and 4 as first fixations and fixations 3 and 5 as refixations. Thus, neither of these studies analyzed precursor fixations.

The largest problem of cognitive EEG research in natural viewing behavior is overlapping EEG activity evoked by sequential saccades. Since eye-movement related EEG responses last longer than the respective fixation durations, the EEG response evoked by one saccade does not have time to fade out before the next one and overlaps with it. Moreover, low-level characteristics of eye movement may affect EEG, such as the effect of saccade size on lambda wave amplitude (Dimigen et al., 2009; Kazai & Yagi, 1999; Thickbroom et al., 1991) or the effect of fixation rank on late FRP amplitude (Fischer et al., 2013; Kamienkowski et al., 2018; Nikolaev et al., 2018). Both types of effects may be systematic and may distort, mask, or be confused with the effects of the cognitive conditions on EEG (Dimigen et al., 2011; Nikolaev, Meghanathan, & van Leeuwen, 2016).

In our two previous refixation studies described above, we solved this problem by comparing EEG epochs only between conditions that were matched on all relevant eye movement characteristics (Dias, Sajda, Dmochowski, & Parra, 2013; Nikolaev et al., 2016). Matching balances the effects of eye movements on EEG and thus enables robust comparison of eye-movement related EEG between conditions. However, matching involves data loss, because EEG epochs from non-matching eye movement characteristics are excluded from the analysis. Moreover, matching based on absence of statistically significant differences on some eye movement characteristics does not prevent trend contributions from those characteristics (see Dimigen and Ehinger (2021) for more detailed discussion).

Another possible solution to consecutive saccades evoking overlapping EEG activity is based on multiple regression. This technique is similar to the traditional mass-univariate modeling of event-related potentials (ERPs), which was used to adjust for multiple simultaneous discrete and continuous covariates (Smith & Kutas, 2015). However, mass-univariate modeling cannot take into account the fact that, as a result of the variable fixation durations of successive eye movements in unrestricted viewing behavior, the degree of overlap in EEG signals varies. This is because mass-univariate modeling requires segmentation of EEG data relative to a single event (Smith & Kutas, 2015) and has no mechanism to account for EEG activity related to preceding or following events. This was also a shortcoming in our earlier study, where we used generalized additive mixed models (GAMM) of EEG epochs with both experimental conditions and eye movement parameters as covariates (Van Humbeeck, Meghanathan, Wagemans, van Leeuwen, & Nikolaev, 2018).

In multiple regression, deconvolution modeling can take the varying temporal overlap into account by time-expansion of the design matrix for the duration of the continuous EEG (Dimigen & Ehinger, 2021; Ehinger & Dimigen, 2019). This technique estimates unknown isolated neural responses from the measured EEG and the latencies of experimental and eye movement events, in order to correct for overlapping eye movement effects on EEG. Deconvolution modeling also allows us to correct for the nonlinear effects of various eye movement covariates, such as fixation duration and saccade size and angle. This is achieved by a combination of linear deconvolution with nonlinear spline regression, as used in the generalized additive model (GAM) (Wood, 2017). Deconvolution

modeling generates beta coefficients, which represent partial effects for the predictors of interest and correspond to subject-level ERPs in traditional ERP analysis. Then these beta coefficients are adjusted for the eye movement covariates included in the model. The adjusted coefficients allow fixation-related EEG to be compared robustly across different fixation categories – the conditions of our interest. Motivated by recent successful examples of deconvolution modelling in face perception (Gert, Ehinger, Timm, Kietzmann, & König, 2022) and episodic memory formation (Nikolaev, Bramão, Johansson, & Johansson, 2023), we propose an analysis pipeline for EEG research in unrestricted viewing.

Methods

From the dataset used in this study we previously analyzed EEG in stimulus conditions (Van Humbeeck et al., 2018) and also compared EEG related to refixations and ordinary fixations, but not precursor fixations (Nikolaev et al., 2018).

Participants

23 healthy adults (two male) took part in the experiment. Data from two participants were removed: one because of problems during eye movement recording and another because of excessive EEG artifacts. The mean age of the remaining 21 participants was 21.6 (range = 18-33) years. All participants gave written informed consent. The study was approved by the Ethics Committee of the Faculty of Psychology and Educational Sciences of KU Leuven.

Stimuli and procedure

Gabor patches of approximately 0.3-0.4° of visual angle were randomly placed with a mean distance of 0.7° between them in large displays of 30 x 30° at a viewing distance of 55 cm. In half of the trials, at a random location in the display, seven patches formed a contour because their orientation was aligned +/- 25° with the neighboring patches (contour-present trials). In the other half of the trials, the orientation of all patches was random (contour-absent trials).

Participants initiated a trial by pressing the space bar on the computer keyboard. At the beginning of a trial a fixation cross was presented for a random duration between 0.5 and 1 s. Next, a search display was presented for 8 s. Contour-present or contour-absent displays were presented in random order. Participants searched for a contour until the search display disappeared. During a subsequent 5-s response interval, participants indicated the presence or absence of the contour by pressing “p” or “q” keys of the computer keyboard. A feedback screen indicated whether the response was correct. 120 contour-present and 120 contour-absent trials were presented. The trials were organized in 6 blocks of 40 trials with two-minute breaks between blocks. A short practice session preceded the experiment.

Eye movement recording

The display size necessitates the use of eye movements to search for a contour. Eye movements were recorded with a desktop version of the EyeLink 1000 eye tracking system (SR Research Ltd., Ontario, Canada). The sampling frequency was 250 Hz. A chinrest stabilized participant’s head. A 9-point calibration was performed before each block and whenever it was needed during the block, e.g., if participants occasionally moved their head away from the chinrest. The mean number of

calibrations per experiment across participants was 17.7 (range 8-32, SD=7.9). A maximum of 2° error margin between calibration and validation was allowed. The space bar press at the beginning of the trial triggered a drift correction, which allowed tracking errors to be kept within 2°.

EEG recording

EEG was recorded at a sampling rate of 250 Hz using a 256-channel Geodesic Sensor Net (EGI, a Philips company, Eugene, OR, USA). The net included electrodes for recording the vertical and horizontal electrooculogram. The recording reference was Cz. The EEG was filtered online with an analog high-pass filter of 0.1 Hz and a 100-Hz low-pass filter. TTL pulses were sent through a parallel port from the stimulus presentation computer to the eye tracking and EEG systems. The synchronization of EEG and eye movement recordings was performed offline using the EYE-EEG extension (Dimigen et al., 2011) for EEGLAB (Delorme & Makeig, 2004).

Selection of refixations, precursor fixations and ordinary fixations

We only analyzed contour-absent trials with correct responses, because herein only visual search could reasonably be considered to last the full 8 s duration of the trial. In the contour-present trials, search happened only in initial intervals of uncertain lengths, as the discovery of the contour at any moment terminates search and initiates response preparation. Since a contour, if present, invariably received its first fixation within 3 s (Van Humbeeck et al., 2018), the search was likely too short and the number of fixation-related EEG epochs within it insufficient for reliable EEG analysis.

Fixations and saccades were detected in the gaze data using the velocity-based algorithm for saccade detection (Engbert & Mergenthaler, 2006) of the EYE-EEG extension. In each trial, we identified precursor fixations and refixations within a sequence of fixations (Fig. 1). To identify precursor fixations, we selected all fixations that later receive refixations. A refixation was defined as a fixation within a radius of 2° of visual angle from such a previous fixation. A 2° criterion has repeatedly been used in refixation studies (Anderson, Bischof, Laidlaw, Risko, & Kingstone, 2013; Gilchrist & Harvey, 2000; Solman, Allan Cheyne, & Smilek, 2011). It assures that precursor fixation and refixation locations overlap on the fovea. If a refixation occurred within 2° from two or more close (<2°) precursor fixations, we scored it as a refixation only once. We did not consider as refixations any subsequent fixations prior to leaving the 2° range. If a chain of two or more consecutive refixations occurred, we only kept the first precursor fixation and the immediate refixation, and refrained from assigning these epithets to any item in the chain of refixations. We thus avoided any fixations having both a precursor and refixation label and hence any ambiguity in assigning fixation-related EEG to precursor fixations or refixations.

The number of precursor fixations was slightly smaller than that of refixations, as several refixations could originate from the same precursor fixation. Precursor fixations and refixations were distributed unequally in time, skewing towards the left and right edge of a trial, respectively. Precursor fixations and refixations were separated by, on average, 9 (SD = 1.2, range 7-10.9) intervening fixations.

To select ordinary fixations, we excluded precursor fixations and refixations (also the ones discarded in a chain of refixations during the selection) from all the fixations in a trial. We also discarded fixations immediately preceding a refixation because these contain preparatory EEG activity specific for refixations (Nikolaev et al., 2018). All fixations discarded during this selection

procedure were assigned to the category of 'other' fixations. Doing so was necessary for exhaustively modeling all fixations, as we will explain in the Deconvolution section below.

Using the EYE-EEG extension, for each fixation we extracted fixation duration, saccade size and angle, and X and Y fixation positions on the screen. Saccade size and angle correspond to the saccade toward the current fixation. Since differences in viewing behavior may be in evidence, not only in the current fixation but also in the next one, we extracted fixation duration, saccade size and angle for the immediately following eye movement (the duration of the following fixations were included only if they were ordinary or 'other').

EEG cleaning

The EEG data processing consisted of two main parts: cleaning the EEG data, and modelling the overlapping effects of sequential eye movements and their covariates on the EEG. The cleaning was performed on continuous EEG, which is an essential requirement for the application of deconvolution modeling with time expansion for correction of overlapping effects, as these may be produced by all the eye movements and other events in the experiment.

We analyzed 148 of the 256 electrodes (Fig. 3D): 108 electrodes close to the cheeks and neck were removed because they often had poor contact due to the long hair of our mostly female participants, and showed strong muscle artifacts. For cleaning we used functions from the EEGLAB toolbox for MATLAB. First, we applied the *pop_cleanline* function, which removes power line noise from EEG using multi-tapering, and a Thompson *F*-statistic. This method uses a 4-s sliding window (with 1-s step), in which a frequency-domain regression estimates the amplitude and phase of the sinusoidal signal at the power-line frequency (50 Hz) and its harmonics. The fitted signal is subtracted from the EEG. Then we applied *clean_artifacts*, which removes flat-line channels, low-frequency drifts, noisy channels, and short-time bursts. To remove transient or large-amplitude artifacts this function uses artifact subspace reconstruction (ASR). It is an automatic, subspace-based method, which compares the structure of the artifactual EEG activity to that of known artifact-free reference data (Mullen et al., 2015). Artifact-free data from a given EEG recording are obtained by automatically selecting low-variance EEG sections. ASR then calculates a clean subspace based on this activity. Next, ASR projects 1-s sliding windows into this clean subspace, which allows for reconstruction of an artifact-reduced EEG signal. Instead of using such an interpolated signal directly, ASR takes deviations of the reconstructed signal to the raw data as an indication of noise-contamination and marks these portions for rejection. The efficiency of ASR for artifact removal crucially depends on the ASR parameter that defines the tradeoff between removing non-brain signals and retaining brain activities. We set the ASR parameter to 20, which was found to be optimal in a dedicated study (Chang, Hsu, Pion-Tonachini, & Jung, 2020). On average, this procedure removed 10.5 (SD=7.3) channels per participant, but entire EEG segments were not removed, given the crucial requirement to use continuous EEG for deconvolution modeling.

We removed ocular artifacts using the OPTICAT function (Dimigen, 2020). This function was designed with a focus on removing artifacts in unrestricted viewing behavior, particularly saccadic spike activity. Like most artifact removal methods, this function is based on independent component analysis (ICA), but requires preparation of the input EEG, which isolates influences of oculomotor artifacts better than ICA training on unprepared EEG data. The preparation involves high-pass EEG filtering at 2 Hz but no low-pass filtering, to preserve the high-frequency (> 40 Hz)

components of myogenic activity, which are characteristic of the saccadic spike potential (Keren et al. 2010). A key step of the OPTICAT function is overweighting the contribution of saccadic spike activity in the EEG input to ICA. This improves artifact correction, particularly of saccadic spike activity. Overweighting of the filtered data was achieved by cutting 30-ms EEG segments (-20 to +10 ms) around saccade onsets as identified by eye tracking, and repeatedly appending these segments to the EEG. Then, ICA was trained on these overweighted data, and the obtained ICA weights were transferred to the unprepared data. The variance of each independent component during saccade and fixation intervals was calculated. Components with greater variance during saccade than fixation intervals are more likely to reflect ocular artifacts. The ratio between the mean variance during saccade and fixation intervals was computed. If the ratio exceeded 1, the component may already reflect ocular artifacts, but in effect, the ratio threshold was set slightly higher, at 1.1, as this is considered optimal for reducing misclassifications (Plöchl, Ossandón, & König, 2012). The ratio of each independent components was checked against this threshold. If the ratio exceeded this threshold, the corresponding components were considered to be saccade-related and were removed. On average, 4.2 (range 2-7, SD=1.37) saccade-related components per participant were removed. (Fig. S1 shows maps of saccade-related components intended for rejection and the distribution of variance ratio of all components for a representative participant).

Next, the ICs related to the remaining artifacts were removed with the automatic classifier (*pop_iclabel*) (Pion-Tonachini, Kreutz-Delgado, & Makeig, 2019). The probability ranges of independent components to be removed as artifacts were set as follows: muscle .4-1, eye .9-1, heart .05-1, line noise .4-1, channel noise .4-1, other .4-1. On average, 2.7 (range 0-6, SD=1.53) components per participant were removed. The EEG was then recreated without these components. Finally, EEG was filtered with a low cut-off of 0.1 Hz (-6 dB at 0.05 Hz) and with a high cut-off of 30 Hz (-6 dB at 30.05 Hz) using the *pop_eegfiltnew* function with default settings. EEG was re-referenced to average reference. The channels previously removed by *clean_artifacts* were interpolated with spherical spline interpolation.

Deconvolution

Due to the non-uniform distribution of fixation durations, effects of sequential eye movements in natural viewing behavior on EEG are systematic and may confound effects of experimental conditions. Moreover, low-level oculomotor characteristics, such as fixation duration, X and Y positions of a fixation on the screen, the size and angle of saccades, *per se* may affect fixation-related EEG (Cornelissen, Sassenhagen, & Võ, 2019; Dimigen et al., 2011; Nikolaev et al., 2016). In addition, the EEG response evoked by the onset of the stimulus screen may distort the following fixation-related potentials (Dimigen et al., 2011; Gert et al., 2022).

To eliminate these effects, we used the deconvolution approach implemented in the Unfold toolbox for MATLAB (Ehinger & Dimigen, 2019). This approach involves regression-based estimation of ERP (for an in-depth review see Smith & Kutas, 2015). The toolbox performs a regression-based EEG analysis that includes mass univariate modeling, linear deconvolution modeling, and generalized additive modeling. As a result, it computes the partial effects (i.e., the beta coefficients or “regression ERPs, rERPs”) for predictors of interest, adjusted for all other covariates. The analysis with the Unfold toolbox consists of four major steps, which are described in detail in (Ehinger & Dimigen, 2019) and are illustrated with respect to different data types in (Dimigen & Ehinger, 2021).

In a first step, we specified the regression model and generated the design matrix. According to the Wilkinson notation, the model formula was defined as follows:

Fixation: y ~ 1 + Fixation Category + spline(fixation rank, 5) + spline(fixation duration, 5) + spline(current saccade size, 5) + spline (following saccade size, 5) + spline(Y fixation position, 5)
Stimulus: y ~1

The formula indicates that we considered multiple effects of the fixation event and the stimulus onset event. Specifically, for fixations, we considered as covariates the fixation onset (y ~ 1, i.e., the intercept) and Fixation Category as a categorical predictor. We used treatment (dummy) coding with 'other' fixations as the reference level (intercept). As a result, all fixation categories (precursor fixations, refixations, and ordinary fixations) were coded as differential FRPs relative to 'other'. The inclusion of 'other' fixations allowed us to account for the overlapping effects on continuous EEG produced at the latencies of 'other' eye movements. The responses to 'other' eye movements could spill over to the responses elicited by the eye movements of interest, because they often interleaved between precursor fixations, refixations, and ordinary fixations. To control for overlapping effects of successive eye movements, we needed to consider all fixations that occurred in the experiment, without exception. Thus, the 'other' fixations constituted an essential level of the predictor 'Fixation Category', even though they were not used in further comparisons. Eye movement covariates were selected for inclusion in the model based on the results of the eye movement analysis, as described below in the section 'Selection of eye movement covariates for deconvolution correction'.

Since we assumed that the selected eye movement covariates have nonlinear effects on EEG, we modeled them with a basis set of five spline predictors. Automatic procedures for estimating the number of splines are currently not available. We followed the recommendation of Dimigen & Ehinger (2021) and set the number of splines to five, thereby limiting the "wiggliness" or un-smoothness of the nonlinear relationship. Spline knots were placed on the participant-specific percentiles of the covariates (i.e., on the 3 ($N_{splines}$-2 = 5-2) quantiles). We did not include interaction between splines in this dataset, as these would have required fitting 2D-splines, raising the number of predictors beyond feasible for the current dataset. We modelled the potentials evoked by the stimulus events using only a single waveform for all images (y ~ 1, i.e., the intercept).

In a second step, the design matrix was time-expanded in the time window between −200 and +500 ms around fixation and stimulus onset events, using the function *uf_timeexpandDesignmat* of the Unfold toolbox, in which 175 'local' time points around each event are added as predictors (175 points due to a sampling rate of 250 Hz and 700 ms duration). The total number of predictors before time-expansion was 25. This number is the sum of one intercept, four categorical predictors relating to the fixation categories, and five eye movement (and fixation rank) predictors modelled with five splines (i.e., 5*$N_{splines}$-1 = 20, per spline we remove one parameter, similar to when modeling the categorical predictor in the presence of an intercept). Per event type, the time expansion takes the respective mass-univariate design-matrix (number of events x 25 predictors) and generates a new design matrix applicable to the continuous EEG (see Fig. 4 in Dimigen and Ehinger (2021) for an illustration of time-expansion). Each event is modelled by a set of time-lagged impulse response functions, one for each time lag, – weighted by its respective mass-univariate design-matrix value. These values are pasted into the new design matrix around the onset of the respective event. Because this new design matrix is defined for all time points of the continuous EEG, we estimate only a single linear model instead of estimating one linear model per time-point,

as in the mass univariate approach. This allows us to simultaneously estimate all stimulus and fixation betas, accounting for their potential overlap effects. The time-expanded design matrix spanned the duration of the entire EEG recording. It had 4375 (25 predictors x 250 Hz x 0.7 s) columns. The number of rows varied across participants because of the different number of events (on average 1,343,503 (range 1,076,301-1,773,579, SD=206,900) rows per participant). Thus, for 4375 parameters, we obtained approx. 1,340,000 data points. Since the number of data points per parameter exceeds the number of parameters by two orders of magnitude, the model is not over-parameterized.

In the third step, we excluded irrelevant intervals from modeling by setting entire rows of the time-expanded design matrix to zero, using the function *uf_continuousArtifactExclude*. Filling with zeros preserved the timing of continuous EEG. Particularly, we removed from the model the inter-trial intervals, the breaks between blocks, the contour-present trials, the trials with incorrect responses, the trials without refixations, and bad eye-tracking intervals. Then, the deconvolution model was fitted (*uf_glmfit*) for each of the 148 electrodes using the iterative Least Squares Minimal Residual algorithm (Fong & Saunders, 2011) for sparse design matrices.

In the fourth and final step, we reconstructed averaged EEG waveforms ("regression-based fixation-related potentials", rFRPs) from the beta coefficients of the model for the three fixation categories for each participant using the functions *uf_predictContinuous* and *uf_addmarginal*. In principle, the raw beta coefficients could be interpreted and compared statistically, since they represent the "pure" effects of the predictors. These effects may be considered as a rough analog of difference waves relative to a reference level. Accordingly, the waveforms of the "pure" effects have highly wiggly shapes, similar to ERP difference waves. This complicates the comparison of deconvolutional and traditional ERP results. We addressed this issue by adding a model intercept to the difference wave. But since we used nonlinear modeling with splines, there was no clear reference level for the nonlinear basis set (the set that transforms predictor values by weighting beta coefficients). Therefore, we estimated all nonlinear effects at the corresponding mean predictor levels and added for each fixation category these estimates to the beta coefficients. This ensured that all fixation categories are presented at the same estimated predictor levels. The resulting waveforms were comparable to the participant-level averages in traditional ERP analyses.

Statistical analysis

Deconvolution was performed for each participant separately. In principle, we could compute group-statistics across individual partial-R^2. However, at present, partial-R^2 can only be evaluated for a whole epoch, not on individual time-points. To perform the statistical analysis at the group level, we used a repeated-measures ANOVA on the mean FRP amplitudes in the time windows described below. The Huynh-Feldt correction for p-values associated with two or more degrees of freedom was applied in case of sphericity violation. The Newman-Keuls test was used for post-hoc analyses.

To perform the statistical analysis on the group level we estimated the FRP amplitude in unbiased time windows based on the grand average and *a priori* regions of interest (ROIs). Since the number of *a priori* tests is typically small, the issue of multiple comparisons for them is minor, which increases the statistical power of the tests. Moreover, they are more likely to detect narrowly distributed effects that occur across a small number of time points and electrodes (Groppe, Urbach, & Kutas, 2011). We selected eight ROIs over the left and right hemisphere, namely, frontal, central,

parietal and occipital brain regions, which were defined around landmark electrodes of the International 10-20 System of Electrode Placement: F3, F4, C3, C4, P3, P4, O1, O2 (the inset in Fig. 3D). For each ROI, we averaged amplitudes over one central and six surrounding electrodes. This approach involved 56 (=7 x 8) electrodes, symmetrically and systematically distributed over the head. Such an approach is generally suggested for high-density electrode montages (Dien & Santuzzi, 2005). Based on visual inspection of the grand-averaged FRPs we selected two time windows. The first, lambda, time window included 30-130 ms after fixation onset, which was chosen as the 100 ms window centered on the lambda peak latency of 80 ms, a latency which was found by averaging across all conditions and participants. The second, late, time window was chosen to include the most pronounced FRP negativity over the occipital regions 200-400 ms after fixation onset.

For the FRP amplitude in the lambda time window, we considered only the occipital ROIs (OL and OR) because here the lambda activity is maximal (Kazai & Yagi, 2003; Thickbroom et al., 1991; Yagi, 1979). Therefore, the ANOVA had two factors: Fixation category (Precursor Fixation, Refixation, Ordinary Fixation) and Hemisphere (left, right). For the late time window, we considered all 8 ROIs, and therefore the ANOVA had three factors: Fixation category (Precursor Fixation, Refixation, Ordinary Fixation), ROI (frontal, central, parietal, occipital), and Hemisphere (left, right). The statistical analyses were performed with STATISTICA 10 (StatSoft Inc., Tulsa, OK, USA) and R version 4.2.0 (2022).

Results

Eye movement results

There were on average 205 (range 130-270, SD=39.9) precursor fixations, 219 (range 138-286, SD=45) refixations, 1680 (range 1266-2347, SD=284.5) ordinary fixations, and 402 (range 246-597, SD=103) ‘other’ fixations per participant.

For fixation duration, a repeated-measures ANOVA with the factors of Fixation category (precursor fixations, refixations, ordinary fixations) and Fixation order (current vs following fixation) showed an effect of Fixation category ($F(2, 40) = 6.8$, $p = .005$, $\varepsilon = .87$), Fixation order ($F(1, 20) = 10.9$, $p = .004$), and an interaction between them ($F(2, 40) = 19.5$, $p < .001$, $\varepsilon = .92$) (Fig. 2A). Post-hoc tests revealed no difference in duration between fixation categories of the current eye movement (all $p > .4$), but differences in duration between all categories of the following eye movement (all $p < .002$): average duration of fixations following refixations was longest while those following precursor fixations were shortest (Fig. 2A). Moreover, precursor and ordinary fixations had longer durations than fixations following them (all $p < .04$), while the duration did not differ between refixations and their following fixations ($p = .22$). For saccade size, an ANOVA with the same design showed an effect of Fixation category ($F(2, 40) = 14.9$, $p < .001$, $\varepsilon = .98$), Fixation order ($F(1, 20) = 11.3$, $p = .003$), and an interaction between them ($F(2, 40) = 47.4$, $p < .001$, $\varepsilon = .86$) (Fig. 1B). Post-hoc tests revealed that saccades were largest in size before precursor fixations and smallest before refixations (all $p < .001$). Following saccades were largest after ordinary fixations and smallest after precursor fixations (all $p < .02$). Among fixation categories, saccade size was largest before precursor fixations and smallest afterwards. Moreover, saccades leading to precursor fixations were larger than saccades following them ($p < .001$). In contrast, saccades leading to refixations and ordinary fixations were smaller than saccades following them (all $p > .04$). For saccade angles, a circular ANOVA (the R package ‘Circular’, v0.4-93; (Lund & Agostinelli, 2017)) on data pooled across

participants showed no significant differences between fixation categories for current ($F(2, 44181) = 1.1$, $p = .3$) or following saccades ($F(2, 44181) = 0.5$, $p = .6$) (Fig. 2G). Fixation positions were compared between fixation categories separately for X and Y positions. No effect of fixation categories on the X fixation position was found ($F(2, 40) = 0.7$, $p = .47$). For the Y position, we found an uncorrected effect of fixation categories ($p = .025$) which, however, lost significance after Huynh-Feldt correction: ($F(2, 40) = 4.04$, $p = .052$, $\varepsilon = .56$) (Fig. 2E). Nevertheless, we performed a post-hoc test and found that the Y position of ordinary fixations differed from that of refixations ($p = .04$) and precursor fixations ($p = .02$) (as expected, positions of refixations and precursor fixations were about the same ($p = .83$)).

Our results show changes in oculomotor behavior characteristic of precursor fixations: a decrease in duration and saccade size of the following fixation, which fails to occur for refixations and ordinary fixations. Moreover, size of current and following saccades and Y fixation positions differ between fixation categories. These differences may confound FRP effects associated with fixation categories and should be corrected before further analysis.

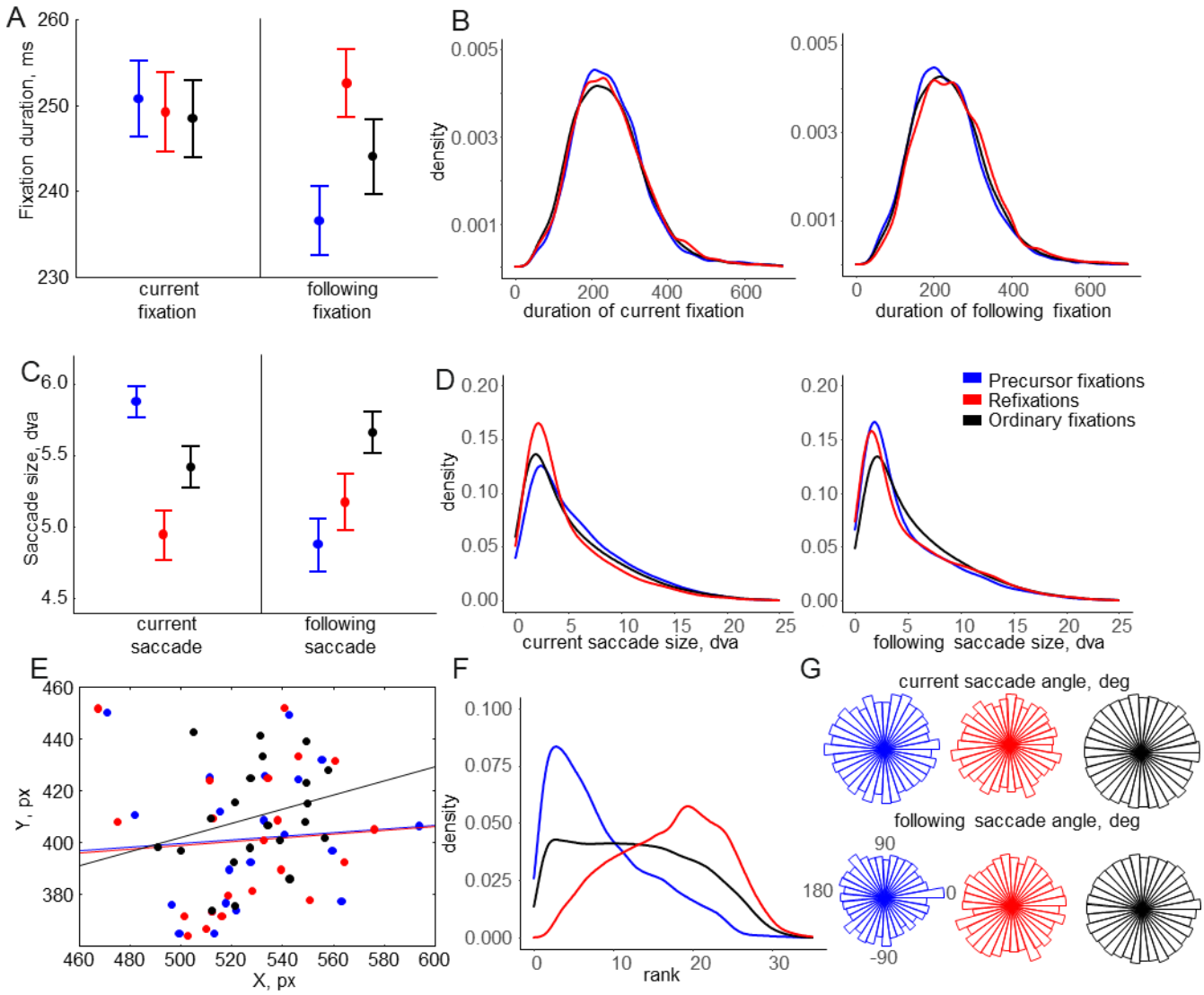

Fig. 2. Eye movement results for three fixation categories. A: Duration of the current and following fixations (mean-error plots, with error bars indicating the standard errors of the means across 21 participants). B: Probability density estimation of the corresponding fixation durations. C: Size of the current and following saccades. D: Probability density estimation of the corresponding saccade sizes. E: Distribution of mean fixation positions on the screen for each

participant (each dot represents one participant). The lines indicate the linear fits of the distributions, emphasizing the difference in the Y position of ordinary fixations. F: Probability density estimation of the fixation rank within an 8-s trial. G: Distribution of angles of the current and following saccades.

EEG results

Selection of eye movement covariates for deconvolution correction

Differences between eye movements during unrestricted viewing could have an effect on EEG confounding that of the conditions of interest (Dimigen et al., 2011; Nikolaev et al., 2016). To correct these confounds, we applied deconvolution modeling. Our inclusion criterion for deconvolution correction of eye movement covariates was the presence of a difference between fixation categories as observed in the eye movement analysis. We included the fixation rank, i.e., the position in the order of fixations within a trial, because it differed between precursor fixations and refixations by definition (Fig. 2F). Moreover, it is known that the amplitude of fixation-related potentials during a trial with multiple eye movements depends on the fixation rank (Fischer et al., 2013; Kamienkowski et al., 2018; Nikolaev et al., 2018). We included the size of current and following saccades, which differed between fixation categories (Fig. 2C), but we did not include saccade angles, since they did not differ. We also included the Y fixation position, which was marginally different between fixation categories (Fig. 2E). Finally, we included the duration of the current fixation. Though this duration did not differ between fixation categories, it is indicative of the onset latency of following saccades. The average (across all categories) duration in our task was 247 ms, and thus most of subsequent eye movements occurred in the middle of the late time window (200-400 ms after fixation onset). Saccadic-related potentials evoked by following eye movements may interfere with ongoing FRPs in this time window, especially given that following saccades differ in size between conditions.

Selection of a baseline interval

In EEG research, an ideal baseline interval should contain no traces of evoked or induced EEG activity. Therefore, in a stimulus-response paradigm with fixed eye movements, the preferred baseline interval is usually the one before the stimulus onset. The EEG co-registered with unrestricted eye movements, however, consists of overlapping brain responses evoked by consecutive saccades. This makes it difficult to find a baseline interval that would be neutral in relation to the fixation-related EEG epoch. We have previously described several options for locations of the baseline interval for fixation-related epochs during unrestricted viewing (Nikolaev et al., 2016). For example, a common baseline could be selected before the onset (stimulus presentation) of a trial involving multiple eye movements, for application to each fixation-related epoch of that trial; alternatively, an individual baseline could be selected from some interval around a saccade and applied to the rest of the fixation-related epoch. All options have their pros and cons, and the final choice of baseline depends on the goals and design of the study. However, it is obvious that the baseline interval used should not be affected by the experimental conditions of interest, otherwise baseline correction would transfer to the baseline FRP difference between conditions for the rest of the fixation-related EEG. Consequently, in this study we checked for a difference between the fixation categories in the two candidate baseline intervals.

The first candidate baseline interval was chosen from -200 to -100 ms before fixation onset; an interval that precedes and thus excludes effects of saccade execution. The second candidate baseline interval was chosen from 0 to 20 ms after fixation onset. This interval was considered already free from the influence of saccade preparation and execution, while the perception-related

EEG response has not yet begun (Rama & Baccino, 2010). We applied a repeated-measures ANOVA with factors of Fixation category (Precursor fixation, Refixation, Ordinary fixation), ROI (frontal, central, parietal, occipital), and Hemisphere (left, right) on the mean amplitude in these intervals of the deconvolved but not baseline-corrected FRPs. For the first interval, we found an interaction of Fixation category with ROI ($p = .03$), which, however, lost significance after Huynh-Feldt correction: ($F(6, 120) = 2.4$, $p = .1$, $\varepsilon = .38$), and a triple interaction of Fixation category x ROI x Hemisphere ($p = .02$), which also lost significance after Huynh-Feldt correction: ($F(6, 120) = 2.7$, $p = .06$, $\varepsilon = .43$). For the second interval, we found no main effect or interactions involving Fixation category. Although the interactions for the first interval were not significant, they may suggest a trend for the effect of Fixation category on EEG. Therefore, in all our further EEG analyses we opted for the second interval as our baseline interval.

The effect of fixation categories on FRP

Fig. 3A shows the beta coefficients (FRPs) obtained after deconvolution and adding covariates to the fully adjusted model, grand-averaged across 21 participants in the three fixation categories. The shape of the waveforms is similar to that expected in traditional FRPs time-locked to the fixation onset and is characterized by a prominent lambda wave over the occipital regions. To examine the effect of fixation categories on these FRPs, we applied an ANOVA on the mean amplitude in the lambda and late time windows.

In the lambda time window (30-130 ms after fixation onset), there was neither a main effect of Fixation category on the FRP amplitude, nor an interaction with Hemisphere (left, right) (both $p > .49$). However, the FRP amplitude was significantly higher over the right than over the left occipital ROIs ($F(1, 20) = 12.5$, $p = .002$).

In the late time window (200-400 ms after fixation onset), the FRP amplitude for precursor fixations was visually different from other fixation conditions, with a maximal difference at approximately 250 ms after the fixation onset (Fig. 3A). This was supported by a significant main effect of Fixation category ($F(2, 40) = 3.3$, $p = .048$, $\varepsilon = 1$) (Fig. 3B). Post-hoc tests showed a difference in FRP amplitude between precursor and ordinary fixations ($p = .045$) and a near-significant difference between precursor fixations and refixations ($p = .06$). The difference for precursor fixations was most prominent over the occipital ROIs, as evidenced by the interaction between Fixation category and ROI ($F(6, 120) = 3.7$, $p = .03$, $\varepsilon = .37$) (Fig. 3C). Post-hoc tests revealed a lower FRP amplitude over the occipital ROIs for the precursor fixations compared with refixations ($p < .001$) and ordinary fixations ($p = .015$), and no difference between refixations and ordinary fixations ($p = .21$).

Topographical maps for 148 electrodes showed a positive peak, equally large for all three fixation categories. The peak was narrowly localized over the occipital areas 100 ms after the fixation onset – the lambda wave (Fig. 3D). At 300 ms after fixation onset, a prominent negativity was spread over the parieto-occipital areas and was mirrored over the frontal areas. The area of negativity over the parieto-occipital areas was larger for precursor fixations than for refixations and ordinary fixations. The difference maps in Fig. 3D show the topography of the FRP difference between precursor fixations and refixations, which was largest among the fixation categories. Thus, the FRPs for precursor fixations differed from FRPs for refixations and ordinary fixations over the occipital areas.

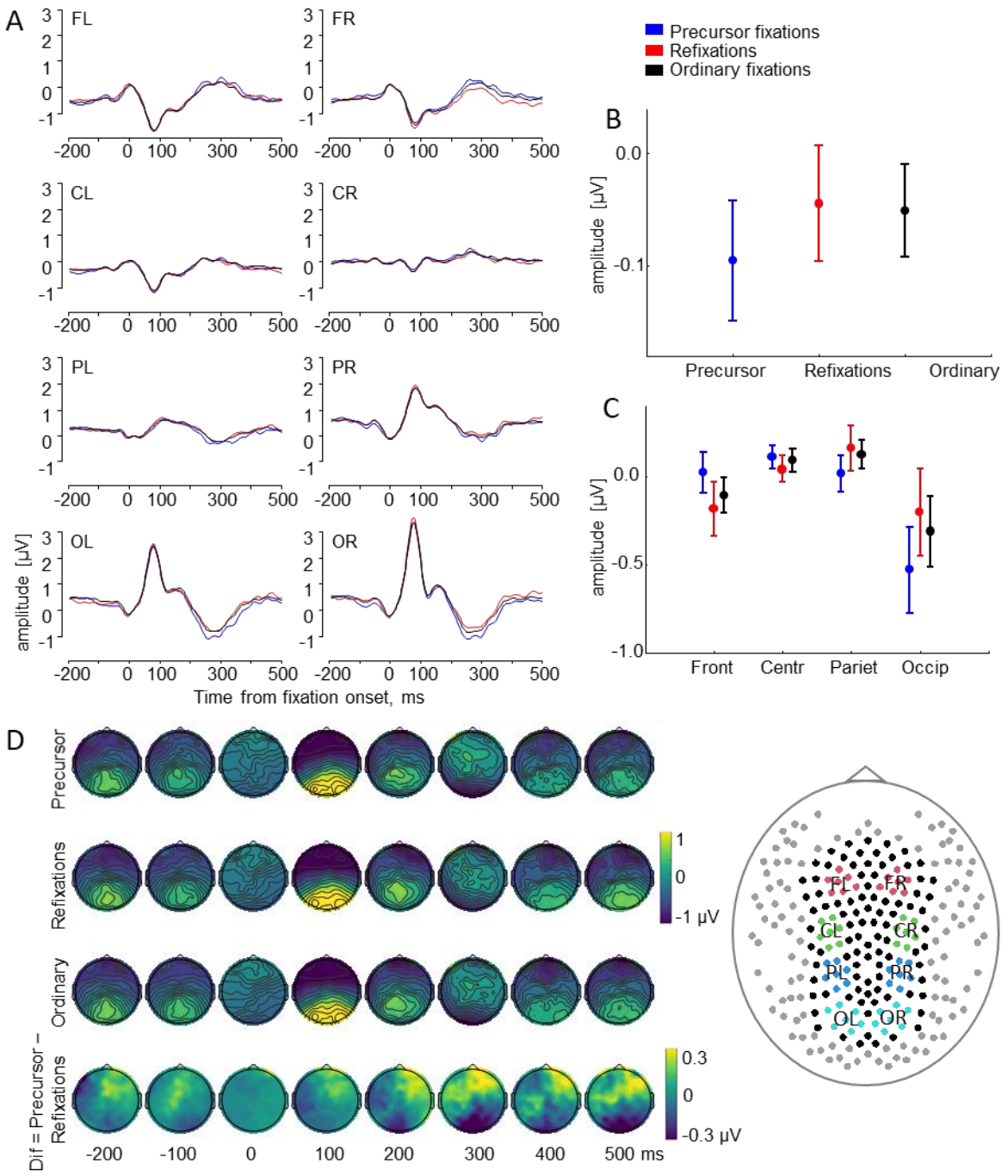

Fig. 3. Fixation-related potentials (regression betas) time-locked to the fixation onset for three fixation categories. The potentials are grand-averaged (N=21) and baseline-corrected at 0-20 ms after fixation onset. A: Fixation-related potentials for 8 ROIs. B: Mean amplitude in the interval 200-400 ms after fixation onset, indicating a main effect of fixation category. C: Mean amplitude in the interval 200-400 ms after fixation onset, indicating an interaction between fixation category and ROI. Error bars indicate standard errors of the means across 21 participants. D: Momentary maps over 148 electrodes for the three fixation categories, as well as a difference map obtained by subtracting FRP of refixations from those of precursor fixations. The inset on the right indicates the locations of all 256 recorded electrodes. Removed electrodes are shown in grey and remaining ones either in black or in different colors according to regions of interest (ROIs): left and right frontal (FL, FR), central (CL, CR), parietal (PL, PR), occipital (OL, OR).

Discussion

We investigated precursor fixations in eye movement: fixations on locations to which the eyes return during later visual exploration. We analyzed co-registered eye movements and EEG from a free-viewing contour-search task, comparing oculomotor and neural properties of precursor fixations with those of refixations and ordinary fixations (which are neither precursor fixations nor refixations). We applied regression-based deconvolution modeling to correct fixation-related potentials (FRPs) for effects of multiple eye movement covariates and for overlapping effects of successive eye movements naturally occurring in unrestricted viewing.

Fixation categories did not affect the lambda activity, which is known to reflect early perceptual processes at each fixation (Dimigen et al., 2009; Kazai & Yagi, 1999; Ossandón et al., 2010; Thickbroom et al., 1991). Specifically, lambda activity is considered a response of the visual cortex to retinal image displacement following eye movement (Dimigen et al., 2009; Kazai & Yagi, 1999; Thickbroom et al., 1991), which has a sensitivity profile and cortical sources similar to the P1 component in event-related potentials (Kazai & Yagi, 2003).

Fixation categories, however, had an influence on late FRP. The FRP of precursor fixations differed in amplitude from ordinary fixations and refixations 200-400 ms after fixation onset, most noticeably over the occipital areas. Since this difference was observed after correcting the EEG for eye movement covariates, it cannot be understood as an oculomotor effect. Thus the effect is likely to reflect distinct sampling of visual information at precursor fixations.

The evoked component affected by fixation categories occurs in the late time window. It may therefore reflect high-order processes accompanying visual sampling in a sequence of eye movements. In particular, the window (250-400 ms after fixation onset) is close to one that previously showed a dependence of FRP amplitude on fixation rank in a free-viewing visual search task (Kamienkowski et al., 2018). This dependency was associated with *integrative* cognitive processes taking prominence as search progresses. Perception in unrestricted viewing behavior involves sampling via eye movements and accumulating information from multiple locations of a visual scene (Hollingworth & Henderson, 2002; Melcher & Kowler, 2001; Tatler, Gilchrist, & Rusted, 2003). Representations of these locations are stored in visual short-term memory for further use (Higgins & Rayner, 2015; Irwin & Zelinsky, 2002; Prime, Vesia, & Crawford, 2011). Some of these may be marked in order to return to them later.

In this process, refixations are aimed at restoration of deficiencies arising in information processing and storage across eye movements. For example, refixations are involved in recovering information that was missed or has become lost during scanning (Gilchrist & Harvey, 2000), updating the representation of a previously visited location (Tatler et al., 2005); rehearsal of a fading memory representation (Meghanathan, Nikolaev, & van Leeuwen, 2019; Zander, Gaertner, Kothe, & Vilimek, 2011); or compensating for a premature shift of attention away from the fixation (Gilchrist, North, & Hood, 2001; Peterson, Kramer, Wang, Irwin, & McCarley, 2001). Thus, the brain processes that distinguish refixations and precursor fixations are likely related to visual short-term memory. The predominance of fixation category effects over the occipital areas is consistent with evidence that the primary visual cortex and other early visual areas in the occipital lobe support the representation and accuracy of short-term memory information (Emrich, Riggall, Larocque, & Postle, 2013; Sligte, Scholte, & Lamme, 2009).

In our contour integration task, precursor fixations followed the largest saccades compared to other fixation categories. It is well known that large saccades after the sudden appearance of a visual stimulus characterize the beginning of a free-viewing trial, while saccade size decreases later in a trial. This reflects the transition from an ambient, exploratory to a focal, scrutinizing viewing mode (Fischer et al., 2013; Pannasch, Helmert, Roth, Herbold, & Walter, 2008; Unema, Pannasch, Joos, & Velichkovsky, 2005). The large saccades leading to precursor fixations may serve to mark locations in the visual stimulus that should be remembered for future revisits. Perhaps these locations contain an abundance of strategic information and therefore give rise to a plan to return later. Accordingly, Wilming and colleagues (2013) found precursor fixation locations to be more visually salient and fixated longer than ones the eyes do not return to. However, fixation durations did not differ between fixation categories. This observation seems to exclude Wilming's saliency hypothesis, but also the opposite hypothesis, that the eye returns to precursor locations because of a deficit in information uptake; in that case we would have expected precursor fixations to last shorter rather than longer. We might therefore consider the possibility that information uptake at precursor fixations differs qualitatively rather than quantitatively from other fixations (neither more nor less, but different). At the beginning of visual exploration, strategic locations may be spotted at the periphery and reached by large saccades. To build the exploration plan, information encoding during precursor fixations may operate in an ambient, as opposed to a focal mode (Fischer et al., 2013; Pannasch et al., 2008; Unema et al., 2005).

This mode may be reflected in the amplitude enhancement of the late FRP component for precursor fixations compared to refixations and ordinary fixations. Thus, precursor fixations may be pivotal moments in ongoing viewing, whose locations are encoded to preserve nodes of the visual scene for further visual exploration. The size of the saccades following the precursor fixations is much smaller than that of the preceding saccades (and is the smallest among the fixation categories) (Fig. 2C). This suggests that between these saccades, a shift may have occurred from an ambient, holistic mode to a focal, analytic mode of perception. Once in this mode, fixation duration is now short (Fig. 2A) and saccade size is small, meaning that the region around the precursor fixation becomes subject to extensive scrutiny, consistently with Wilming and colleagues (2013). Such rapid shifts from holistic to analytic modes of processing are well-documented in the perception of complex visual stimuli (Fitousi, 2020; Navon, 1977; Van Leeuwen & Bakker, 1995).

Our findings extend the understanding of the aforementioned transition from an exploratory to a scrutinizing viewing mode (Fischer et al., 2013; Pannasch et al., 2008; Unema et al., 2005): such transitions may occur repeatedly during visual exploration. In an EEG-eye movement co-registration study, Fischer and colleagues (2013) observed more negative parieto-occipital FRP amplitude for early than for late fixations in a trial, after 250 ms from fixation onset, although they did not analyze this effect statistically. In the same interval, we found a more negative occipital FRP amplitude for precursor fixation than refixations. Both findings are remarkably similar (cf. their Fig. 2A and our Fig. 3A) and are established here as a recurrent feature of lasting visual exploration.

Our study is the first to investigate the neural correlates of the three main categories of eye movements typical for unrestricted viewing behavior, which is characterized by repetitive gaze returns. The importance of refixations for goal-directed visual exploration is nowadays increasingly appreciated. This is supported by experimental studies that show the critical role of refixations in memory formation and retrieval in natural viewing (Kragel & Voss, 2022), as well as by major modelling projects that aim to simulate refixation sequences similar to those observed in multiple

human and animal gaze datasets (Zhang et al., 2022). Our contribution to this research is limited to one particular task: contour integration in dense fields of equidistant and similar Gabor elements. It remains to be seen how our results generalize to different perceptual tasks. We have not attempted to relate precursor fixations to the peculiarities of the current task and to the properties of the visual scene and, whose competing influences are known to control eye movements (Tatler, Hayhoe, Land, & Ballard, 2011). Consequently, future research should explore the neural correlates of precursor fixations in natural scenes containing a broad spectrum of spatial frequencies and visual saliences and should be designed to analyze in more detail the brain processes around precursor fixations. Still, this research will have to take into account the overlapping effects that sequential eye movements produce on brain activity during unrestricted viewing. Our study shows that deconvolution modeling offers a robust solution of this problem. This can be concluded, in particular, from the successful elimination of the saccade size effect on the lambda peak between fixation categories, as the lambda peak is known to be very sensitive to differences in saccade size (Dimigen et al., 2009; Kazai & Yagi, 1999; Thickbroom et al., 1991), such as between our fixation categories.

The analytical pipeline used in this study provides several methodological advances for reliable deconvolution applications:

- The first step involves the use of modern EEG cleaning techniques (e.g., ASR), which can be applied to the continuous EEG required for deconvolution.
- The second step involves the application of ocular artifact removal techniques, such as OPTICAT, that are optimized for the abundance of eye movement artifacts characteristic of unrestricted viewing.
- The third step involves a careful selection of eye movement covariates and other predictors potentially confounded with conditions of interest, which have to be corrected by deconvolution. Our inclination might be to account for as many of these predictors as possible. But this approach is limited on theoretical grounds (e.g., collider bias) and practical grounds (e.g., overfit) . The former cannot be easily resolved without explicit causal modelling (Rohrer, 2018), but overfitting can be diagnosed by investigating the number of iterations of the solver or by cross validation, and remedied by simplifying the model, for instance, by reducing the number of predictors. Data-driven selection of predictors may apply our current strategy to statistically test eye movement and other covariates for effects in the conditions of interest and use only those for which the effect is significant. We currently only tested for effects on the means. This strategy comes with limitations. Due to a possible non-linearity in the EEG response to eye movement covariates, differences may be present also in the distribution, which should also be tested. In a future scenario, the selection could be based on a-priori considerations based on the availability of a theory.
- The fourth step involves a decision about the selection of a baseline interval. This is problematic in natural viewing, because the EEG consists of overlapping brain responses to consecutive saccades. When baseline correction is necessary, we suggest testing the mean EEG amplitude of the candidate baseline intervals for an effect of the conditions of interest and choosing an interval for which no differences could be found. As this amounts to accepting a null-hypothesis, this is only a heuristic. More advanced procedures, such as baseline regression (Alday, 2019), are not currently compatible with overlap correction.

Conclusions

Eye movements do not simply supply our vision with information or passively reflect the outputs of visual processing, but are themselves an inextricable part of the attention and memory brain systems (Awh, Armstrong, & Moore, 2006; Gottlieb, 2012; Voss, Bridge, Cohen, & Walker, 2017). Our study extends this understanding by showing the difference between the three basic categories of fixations in naturalistic viewing behavior. Precursor fixations to locations that are subsequently refixated have distinct neural correlates compared to refixations and ordinary fixations. While the neural mechanisms of refixations have been investigated earlier (Kragel, Schuele, VanHaerents, Rosenow, & Voss, 2021; Meghanathan et al., 2020; Nikolaev et al., 2018), as far as we know, the neural mechanisms of the precursor fixations have not been studied before. Their peculiarity may arise from the combined contribution of cognitive factors responsible for making a strategic plan of visual exploration, and oculomotor factors that determine the size of saccades depending on their serial position (rank) in a trial. These findings emphasize the intertwined character of cognitive processing and oculomotor behavior.

Acknowledgments

ARN and RNM were supported by an Odysseus grant (G.0003.12) from the Flemish Organization for Science (FWO) to Cees van Leeuwen. ARN was also supported by a grant from the Marcus and Amelia Wallenberg Foundation (MAW2015.0043) to Mikael Johansson. BE was funded by Deutsche Forschungsgemeinschaft (DFG, German Research Foundation) under Germany´s Excellence Strategy – EXC 2075 – 390740016. We thank Nathalie Van Humbeeck and Johan Wagemans for permission to use the jointly collected data in this study. We thank Olaf Dimigen for his help with OPTICAT and in synchronizing EEG and eye movement recordings with the EYE-EEG extension for EEGLAB.

References

Alday, P. M. (2019). How much baseline correction do we need in ERP research? Extended GLM model can replace baseline correction while lifting its limits. *Psychophysiology, 56*(12), e13451.

Anderson, N. C., Bischof, W. F., Laidlaw, K. E., Risko, E. F., & Kingstone, A. (2013). Recurrence quantification analysis of eye movements. *Behavior research methods, 45*(3), 842-856.

Awh, E., Armstrong, K. M., & Moore, T. (2006). Visual and oculomotor selection: links, causes and implications for spatial attention. *Trends in cognitive sciences, 10*(3), 124-130.

Beck, M. R., Peterson, M. S., & Vomela, M. (2006). Memory for where, but not what, is used during visual search. *Journal of Experimental Psychology: Human Perception and Performance, 32*(2), 235-250.

Chang, C. Y., Hsu, S. H., Pion-Tonachini, L., & Jung, T. P. (2020). Evaluation of Artifact Subspace Reconstruction for Automatic Artifact Components Removal in Multi-Channel EEG Recordings. *IEEE Transactions on Biomedical Engineering, 67*(4), 1114-1121.

Coco, M. I., Nuthmann, A., & Dimigen, O. (2020). Fixation-related Brain Potentials during Semantic Integration of Object-Scene Information. *Journal of Cognitive Neuroscience, 32*(4), 571-589.

Cornelissen, T., Sassenhagen, J., & Võ, M. L. (2019). Improving free-viewing fixation-related EEG potentials with continuous-time regression. *Journal of Neuroscience Methods, 313*, 77-94.

Delorme, A., & Makeig, S. (2004). EEGLAB: an open source toolbox for analysis of single-trial EEG dynamics including independent component analysis. *Journal of Neuroscience Methods, 134*(1), 9-21.

Devillez, H., Guyader, N., & Guerin-Dugue, A. (2015). An eye fixation-related potentials analysis of the P300 potential for fixations onto a target object when exploring natural scenes. *Journal of vision, 15*(13), 20.

Dias, J. C., Sajda, P., Dmochowski, J. P., & Parra, L. C. (2013). EEG precursors of detected and missed targets during free-viewing search. *Journal of vision, 13*(13), 13.

Dien, J., & Santuzzi, A. M. (2005). Application of repeated measures ANOVA to high density ERP datasets: A review and tutorial. In T. C. Handy (Ed.), *Event-related potentials: A methods handbook* (pp. 57–82). Cambridge, MA: MIT Press.

Dimigen, O. (2020). Optimizing the ICA-based removal of ocular EEG artifacts from free viewing experiments. *Neuroimage, 207*, 116117.

Dimigen, O., & Ehinger, B. V. (2021). Regression-based analysis of combined EEG and eye-tracking data: Theory and applications. *Journal of vision, 21*(1), 3.

Dimigen, O., Sommer, W., Hohlfeld, A., Jacobs, A. M., & Kliegl, R. (2011). Coregistration of eye movements and EEG in natural reading: analyses and review. *Journal of Experimental Psychology: General, 140*(4), 552-572.

Dimigen, O., Valsecchi, M., Sommer, W., & Kliegl, R. (2009). Human microsaccade-related visual brain responses. *Journal of Neuroscience, 29*(39), 12321-12331.

Ehinger, B. V., & Dimigen, O. (2019). Unfold: an integrated toolbox for overlap correction, non-linear modeling, and regression-based EEG analysis. *PeerJ, 7*, e7838.

Emrich, S. M., Riggall, A. C., Larocque, J. J., & Postle, B. R. (2013). Distributed patterns of activity in sensory cortex reflect the precision of multiple items maintained in visual short-term memory. *Journal of Neuroscience, 33*(15), 6516-6523.

Engbert, R., & Mergenthaler, K. (2006). Microsaccades are triggered by low retinal image slip. *Proceedings of the National Academy of Sciences of the United States of America, 103*(18), 7192-7197.

Fischer, T., Graupner, S. T., Velichkovsky, B. M., & Pannasch, S. (2013). Attentional dynamics during free picture viewing: evidence from oculomotor behavior and electrocortical activity. *Frontiers in systems neuroscience, 7*, 17.

Fitousi, D. (2020). Evaluating the independence of age, sex, and race in judgment of faces. *Cognition, 202*, 104333.

Fong, D. C. L., & Saunders, M. (2011). Lsmr: An Iterative Algorithm for Sparse Least-Squares Problems. *Siam Journal on Scientific Computing, 33*(5), 2950-2971.

Fudali-Czyz, A., Francuz, P., & Augustynowicz, P. (2018). The Effect of Art Expertise on Eye Fixation-Related Potentials During Aesthetic Judgment Task in Focal and Ambient Modes. *Frontiers in psychology, 9*, 1972.

Gert, A. L., Ehinger, B. V., Timm, S., Kietzmann, T. C., & König, P. (2022). WildLab: A naturalistic free viewing experiment reveals previously unknown electroencephalography signatures of face processing. *European Journal of Neuroscience, 56*(11), 6022-6038.

Gilchrist, I. D., & Harvey, M. (2000). Refixation frequency and memory mechanisms in visual search. *Current Biology, 10*(19), 1209-1212.

Gilchrist, I. D., North, A., & Hood, B. (2001). Is visual search really like foraging? *Perception, 30*(12), 1459-1464.

Gottlieb, J. (2012). Attention, learning, and the value of information. *Neuron, 76*(2), 281-295.

Groppe, D. M., Urbach, T. P., & Kutas, M. (2011). Mass univariate analysis of event-related brain potentials/fields I: a critical tutorial review. *Psychophysiology, 48*(12), 1711-1725.

Higgins, E., & Rayner, K. (2015). Transsaccadic processing: stability, integration, and the potential role of remapping. *Attention, perception & psychophysics, 77*(1), 3-27.

Hollingworth, A., & Henderson, J. M. (2002). Accurate visual memory for previously attended objects in natural scenes. *Journal of Experimental Psychology: Human Perception and Performance, 28*(1), 113-136.

Irwin, D. E., & Zelinsky, G. J. (2002). Eye movements and scene perception: memory for things observed. *Perception and Psychophysics, 64*(6), 882-895.

Kamienkowski, J. E., Varatharajah, A., Sigman, M., & Ison, M. J. (2018). Parsing a mental program: Fixation-related brain signatures of unitary operations and routines in natural visual search. *Neuroimage, 183*, 73-86.

Kazai, K., & Yagi, A. (1999). Integrated effect of stimulation at fixation points on EFRP (eye-fixation related brain potentials). *International Journal of Psychophysiology, 32*(3), 193-203.

Kazai, K., & Yagi, A. (2003). Comparison between the lambda response of eye-fixation-related potentials and the P100 component of pattern-reversal visual evoked potentials. *Cognitive, affective & behavioral neuroscience, 3*(1), 46-56.

Körner, C., Braunstein, V., Stangl, M., Schlogl, A., Neuper, C., & Ischebeck, A. (2014). Sequential effects in continued visual search: using fixation-related potentials to compare distractor processing before and after target detection. *Psychophysiology, 51*(4), 385-395.

Körner, C., & Gilchrist, I. D. (2008). Memory processes in multiple-target visual search. *Psychological Research, 72*(1), 99-105.

Kovalenko, L. Y., & Busch, N. A. (2016). Probing the dynamics of perisaccadic vision with EEG. *Neuropsychologia, 85*, 337-348.

Kragel, J. E., Schuele, S., VanHaerents, S., Rosenow, J. M., & Voss, J. L. (2021). Rapid coordination of effective learning by the human hippocampus. *Science Advances, 7*(25).

Kragel, J. E., & Voss, J. L. (2022). Looking for the neural basis of memory. *Trends in cognitive sciences, 26*(1), 53-65.

Lund, U., & Agostinelli, C. (2017). Package 'circular'. *Repository CRAN*, 1-142.

Mannan, S. K., Ruddock, K. H., & Wooding, D. S. (1997). Fixation sequences made during visual examination of briefly presented 2D images. *Spatial Vision, 11*(2), 157-178.

Meghanathan, R. N., Nikolaev, A. R., & van Leeuwen, C. (2019). Refixation patterns reveal memory-encoding strategies in free viewing. *Atten Percept Psychophys, 81*(7), 2499-2516.

Meghanathan, R. N., van Leeuwen, C., Giannini, M., & Nikolaev, A. R. (2020). Neural correlates of task-related refixation behavior. *Vision Research, 175*, 90-101.

Melcher, D., & Kowler, E. (2001). Visual scene memory and the guidance of saccadic eye movements. *Vision Research, 41*(25-26), 3597-3611.

Mullen, T. R., Kothe, C. A., Chi, Y. M., Ojeda, A., Kerth, T., Makeig, S., . . . Cauwenberghs, G. (2015). Real-Time Neuroimaging and Cognitive Monitoring Using Wearable Dry EEG. *IEEE Transactions on Biomedical Engineering, 62*(11), 2553-2567.

Navon, D. (1977). Forest before trees: The precedence of global features in visual perception. *Cognitive Psychology, 9*(3), 353–383.

Nikolaev, A. R., Bramão, I., Johansson, R., & Johansson, M. (2023). Episodic memory formation in unrestricted viewing. *Neuroimage, 266*, 119821.

Nikolaev, A. R., Jurica, P., Nakatani, C., Plomp, G., & van Leeuwen, C. (2013). Visual encoding and fixation target selection in free viewing: presaccadic brain potentials. *Frontiers in systems neuroscience, 7*, 26.

Nikolaev, A. R., Meghanathan, R. N., & van Leeuwen, C. (2016). Combining EEG and eye movement recording in free viewing: pitfalls and possibilities. *Brain and Cognition, 107*, 55-83.

Nikolaev, A. R., Meghanathan, R. N., & van Leeuwen, C. (2018). Refixation control in free viewing: a specialized mechanism divulged by eye-movement related brain activity. *Journal of Neurophysiology, 120*(5), 2311-2324.

Nikolaev, A. R., Nakatani, C., Plomp, G., Jurica, P., & van Leeuwen, C. (2011). Eye fixation-related potentials in free viewing identify encoding failures in change detection. *Neuroimage, 56*(3), 1598-1607.

Ossandón, J. P., Helo, A. V., Montefusco-Siegmund, R., & Maldonado, P. E. (2010). Superposition model predicts EEG occipital activity during free viewing of natural scenes. *Journal of Neuroscience, 30*(13), 4787-4795.

Pannasch, S., Helmert, J. R., Roth, K., Herbold, A. K., & Walter, H. (2008). Visual fixation durations and saccade amplitudes: shifting relationship in a variety of conditions. *Journal of Eye Movement Research, 2*(2), 1-19.

Peterson, M. S., Kramer, A. F., Wang, R. X. F., Irwin, D. E., & McCarley, J. S. (2001). Visual search has memory. *Psychological science, 12*(4), 287-292.

Pion-Tonachini, L., Kreutz-Delgado, K., & Makeig, S. (2019). ICLabel: An automated electroencephalographic independent component classifier, dataset, and website. *Neuroimage, 198*, 181-197.

Plöchl, M., Ossandón, J. P., & König, P. (2012). Combining EEG and eye tracking: identification, characterization, and correction of eye movement artifacts in electroencephalographic data. *Frontiers in human neuroscience, 6*, 278.

Prime, S. L., Vesia, M., & Crawford, J. D. (2011). Cortical mechanisms for trans-saccadic memory and integration of multiple object features. *Philosophical transactions of the Royal Society of London. Series B, Biological sciences, 366*(1564), 540-553.

Rama, P., & Baccino, T. (2010). Eye fixation-related potentials (EFRPs) during object identification. *Visual Neuroscience, 27*(5-6), 187-192.

Ries, A. J., Touryan, J., Ahrens, B., & Connolly, P. (2016). The Impact of Task Demands on Fixation-Related Brain Potentials during Guided Search. *PLoS One, 11*(6), e0157260.

Rohrer, J. M. (2018). Thinking Clearly About Correlations and Causation: Graphical Causal Models for Observational Data. *Advances in Methods and Practices in Psychological Science, 1*(1), 27-42.

Shen, K., McIntosh, A. R., & Ryan, J. D. (2014). A working memory account of refixations in visual search. *Journal of vision, 14*(14).

Sligte, I. G., Scholte, H. S., & Lamme, V. A. (2009). V4 activity predicts the strength of visual short-term memory representations. *Journal of Neuroscience, 29*(23), 7432-7438.

Smith, N. J., & Kutas, M. (2015). Regression-based estimation of ERP waveforms: I. The rERP framework. *Psychophysiology, 52*(2), 157-168.

Solman, G. J., Allan Cheyne, J., & Smilek, D. (2011). Memory load affects visual search processes without influencing search efficiency. *Vision Research, 51*(10), 1185-1191.

Tatler, B. W., Gilchrist, I. D., & Land, M. F. (2005). Visual memory for objects in natural scenes: from fixations to object files. *Quarterly Journal of Experimental Psychology. A, Human Experimental Psychology, 58*(5), 931-960.

Tatler, B. W., Gilchrist, I. D., & Rusted, J. (2003). The time course of abstract visual representation. *Perception, 32*(5), 579-592.

Tatler, B. W., Hayhoe, M. M., Land, M. F., & Ballard, D. H. (2011). Eye guidance in natural vision: reinterpreting salience. *Journal of vision, 11*(5), 5.

Thickbroom, G. W., Knezevic, W., Carroll, W. M., & Mastaglia, F. L. (1991). Saccade onset and offset lambda waves: relation to pattern movement visually evoked potentials. *Brain Research, 551*(1-2), 150-156.

Tyson-Carr, J., Soto, V., Kokmotou, K., Roberts, H., Fallon, N., Byrne, A., . . . Stancak, A. (2020). Neural underpinnings of value-guided choice during auction tasks: An eye-fixation related potentials study. *Neuroimage, 204*, 116213.

Unema, P. J. A., Pannasch, S., Joos, M., & Velichkovsky, B. M. (2005). Time course of information processing during scene perception: the relationship between saccade amplitude and fixation duration. *Visual Cognition, 12*(3), 473-494.

Van Humbeeck, N., Meghanathan, R. N., Wagemans, J., van Leeuwen, C., & Nikolaev, A. R. (2018). Presaccadic EEG activity predicts visual saliency in free-viewing contour integration. *Psychophysiology, 55*(12), e13267.

Van Leeuwen, C., & Bakker, L. (1995). Stroop can occur without Garner interference: strategic and mandatory influences in multidimensional stimuli. *Perception and Psychophysics, 57*(3), 379-392.

Voss, J. L., Bridge, D. J., Cohen, N. J., & Walker, J. A. (2017). A Closer Look at the Hippocampus and Memory. *Trends in cognitive sciences, 21*(8), 577-588.

Wauschkuhn, B., Verleger, R., Wascher, E., Klostermann, W., Burk, M., Heide, W., & Kompf, D. (1998). Lateralized human cortical activity for shifting visuospatial attention and initiating saccades. *Journal of Neurophysiology, 80*(6), 2900-2910.

Wilming, N., Harst, S., Schmidt, N., & König, P. (2013). Saccadic momentum and facilitation of return saccades contribute to an optimal foraging strategy. *PLoS Comput Biol, 9*(1), e1002871.

Wood, S. N. (2017). *Generalized additive models: an introduction with R* (2nd edition ed.). New York: Chapman & Hall/CRC.

Yagi, A. (1979). Saccade size and lambda complex in man. *Physiological Psychology, 7*, 370-376.

Yarbus, A. L. (1967). *Eye movements and vision*. New York: Plenum Press.

Zander, T. O., Gaertner, M., Kothe, C., & Vilimek, R. (2011). Combining eye gaze input with a brain-computer interface for touchless human-computer interaction. *International Journal of Human-Computer Interaction, 27*(1), 38-51.

Zelinsky, G. J., Loschky, L. C., & Dickinson, C. A. (2011). Do object refixations during scene viewing indicate rehearsal in visual working memory? *Memory and Cognition, 39*(4), 600-613.

Zhang, M., Armendariz, M., Xiao, W., Rose, O., Bendtz, K., Livingstone, M., . . . Kreiman, G. (2022). Look twice: A generalist computational model predicts return fixations across tasks and species. *PLOS Computational Biology, 18*(11), e1010654.